Monotonic axial compressive behaviour and confinement mechanism of square CFRP-steel tube confined concrete

Yanlei Wang[1], Gaochuang Cai[2,3]*, Amir Si Larbi[3], Danièle Waldmann[4], Konstantinos Daniel Tsavdaridis[5], Jianghua Ran[1]

1. State Key Laboratory of Coastal and Offshore Engineering, School of Civil Engineering, Dalian University of Technology, Dalian 116024, P.R. China.
2. Dept. of Architecture, Faculty of Eng., Fukuoka University, Fukuoka, 814-0180, Japan.
3. Univ Lyon, Ecole Nationale d'Ingénieurs de Saint-Etienne (ENISE), Laboratoire de Tribologie et de Dynamique des Systèmes (LTDS), UMR 5513, 58 Rue Jean Parot, 42023 Saint-Etienne Cedex 2, France.
4. Laboratory of Solid Structures, University of Luxembourg, Luxembourg, Luxembourg.
5. School of Civil Engineering, University of Leeds, Leeds LS2 9JT, UK

*Corresponding author: Gaochuang Cai
Email: gaochuang.cai@enise.fr

Abstract

Steel tube confined concrete (STCC) is widely used in the vertical members of high-rise buildings such as columns. The axial load is not directly resisted by the steel tube in STCC, but is resisted via the interfacial frictional stress between steel tube and concrete core, which is different with that of concrete filled steel tube (CFT) members and would effectively suppress the outward local buckling of steel tube at early stage. Recently, fibre-reinforced polymer (FRP) confined STCC presents a potential to enhance the ductility and durability of such vertical elements. This paper presents an experimental study on monotonic axial compressive behaviour of carbon FRP (CFRP) confined STCC (CFRP-STCC) stub column and an analytical study on the confinement mechanism of and the ultimate axial bearing capacity of the elements. A three-stage confinement mechanism involving the different contributions of the steel tube and the CFRP wrap in CFRP-STCC elements was proposed based on the test results. A prediction model of the ultimate axial bearing capacity of CFRP-STCC stub columns was developed subsequently. Results show that the presence of CFRP wrap enhances effectively the load-bearing capacity and the ductility of steel tube confined plain concrete and reinforced concrete elements, and significantly prevents the local buckling of the steel tubes in the

elements. The proposed prediction model of ultimate axial bearing capacity assesses test results with a great agreement.

Keywords: FRP confined concrete; Steel tube confined concrete; Constitutive model; Confinement mechanism; axial compressive behaviour

1. Introduction

Reinforced concrete (RC) structures still are widely used in most of the earthquake-prone zones of the world. Numerous studies have revealed that a sufficient confinement can significantly enhance the ductility of RC elements subjected to seismic loads. To achieve an effective confinement, various methods and technical provisions have been developed according to a series of experimental laboratorial studies and earthquake field surveys. Among them, an effective and easily implemented method at the early stage of the previous research is using steel stirrups or hoops with a smaller spacing at the hinge zones of RC elements such as RC columns.

In order to further improve the bearing capacity and seismic performance of RC columns, concrete-filled steel tube (CFT) column (Fig.1a) has been developed and widely applied in civil engineering due to the effective confinement of steel tube in such elements [1]. However, the steel tube of CFT must be thick to avoid its potential local buckling [2]. Steel tube confined concrete (STCC) column (Fig. 1b) is an innovative type of composite columns [3-9], in which the main difference with CFT column is that the steel tube is disconnected to both ends of the column (Fig. 1b). There are two main benefits obtained from this difference of STCC columns. One is the construction simplification of beam-column joints because that steel tube does not need to pass through the joint zone, which has been illustrated by the literature [9]. Another is that the potential local buckling of steel tube can be effectively avoided or delayed as STCC elements are under compressive load. This is because that the steel tube in STCC does not resist directly axial load and mainly provides a confinement to concrete core. It means the thickness of steel tube in STCC can be controlled compared with that of CFT in order to archive the same load-bearing capacity. The STCC elements have the potential of wide applications in new construction. It should be noted that, however, the steel tube in STCC still resists certain axial load from compressive load via the interfacial friction between steel tube and concrete core. But the interfacial friction can be reduced by smoothing the inner surface of steel tube (i.e. oil treatment). However, the main concerns of CFT and STCC elements are the durability issues of external steel tube (i.e. its resistance to corrosion) when they are subjected to aggressive environments. The conventional corrosion protection for steel tube is additional coating. However, some small defects could occur in the coating process or the use of steel tubes [2] such as cyclic loads or fatigue loads, which then can cause the pitting corrosion of the tube and then result in the subsequently large area corrosion of the steel tube. Therefore, it is desirable to explore alternative corrosion protection for steel tube.

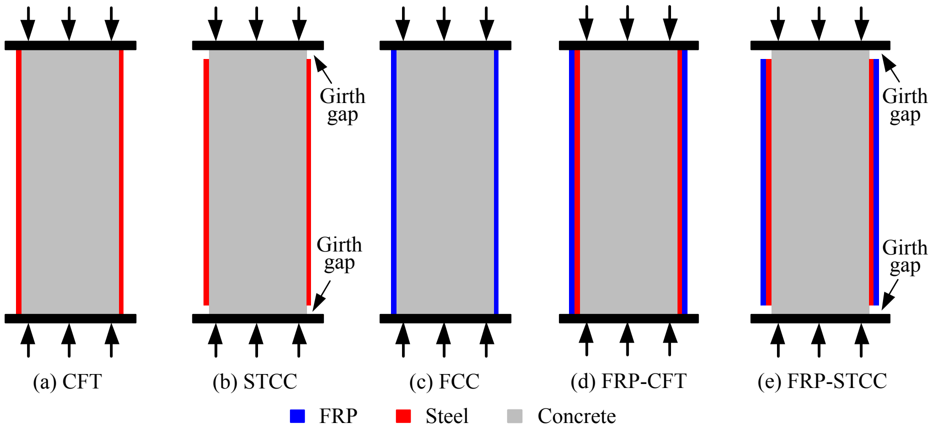

Fig. 1. Schematic diagram of different confined concrete columns.

Fibre reinforced polymer (FRP) has been widely applied in civil engineering due to its high strength, light weight, good fatigue resistance, and especially excellent durability [10-17]. FRP confined concrete (FCC) column (Fig. 1c) is one of important applications of FRP material in civil engineering to improve the bearing capacity and ductility of concrete core [18-19]. FRP material provides a new choice for steel tube to resist corrosion by wrapping FRP layer on the outside of steel tube. To improve the durability of the outer steel tube of CFT and STCC elements under aggressive environments, and to avoid or delay the early age local buckling of steel tube of CFT elements, several researchers proposed using FRP wrap to confine CFT (FRP-CFT, Fig. 1d) [20-28] or STCC (FRP-STCC, Fig. 1e) [29] elements. FRP-CFT and FRP-STCC elements are two innovative composite elements, which benefit the advantages of both CFT and STCC. The outer FRP wrap/confining can effectively prevent the potential corrosion problem of outer steel tube under aggressive environments and enhance the bearing capacity of CFT/STCC. This means that the same bearing capacity still can be reached in the composite elements when the thickness of steel tube is reduced, which can reduce the manufacturing difficulty of thick steel tube. Meanwhile, it also can delay or even avoid the cracking of the welding seam of the steel tube because of the effective confinement of the outer FRP wrap. It should be admitted that the brittle fracture of FRP material at its ultimate state may lead to a sudden failure of FRP-STCC elements, however, the FRP wrap can provide the STCC higher confinement which could significantly improve the bearing capacity and the peak strain of the STCC elements. Due to the large difference of thermal expansivity between FRP and steel, large temperature difference is considered as a challenge for the interface adhesive in FRP-CFT and FRP-STCC elements. This environment may cause the degradation of structural performance of the elements, thus endangers the service life span of the structures. Therefore, high toughness adhesives are suggested to fabricate the FRP wrap in FRP-CFT and FRP-STCC elements to delay the deterioration of their structural behaviours caused by a large temperature difference. Moreover, the balance between the toughness of the adhesives and their glass transition temperatures should be considered, to avoid the serviceability problems of the elements at higher service temperatures due to low glass transition temperature. On the other hand, the aging problem of external FRP wrap due to sunlight (mainly Ultraviolet light) [30], temperature, and humidity is the main concern of the durability of FRP-confined or -strengthened structures. To fix this issue, a surface treatment such as coating of FRP wrap is suggested in practical application. As new corrosion protection of steel, the cost of FRP wrap in FRP-STCC elements is more expensive than those of the conventional corrosion protections of steel, due to the high price of FRP materials and additional coating materials to resist the aging problems of FRP. However, FRP wrap is also expected to improve the structural performance (the bearing capacity, peak strain and local buckling, etc.) of STCC elements with the benefits of the material advantages.

Compared to STCC and FCC elements, limited studies were conducted [2,29,31] to understand the structural behaviour of FRP-STCC elements such as the effectiveness of FRP wrap to prevent the failure provoked by local damage of steel tube. Lin [29] studied the structural behaviour of circular glass FRP (GFRP) confined STCC (GFRP-STCC) columns to investigate the effects of the type of and the number of layers of FRP wrap, stirrup ratio, and loading type. It was reported that FRP wrap, steel tube, and reinforcements in STCC elements all can enhance significantly the axial load-carrying capacity and the ductility of the elements [28]. Huang [31] experimentally investigated the cyclic constitutive behaviour of circular GFRP-STCC columns and proposed a design model to predict the compressive behaviour of the confined concrete. Xu *et al* [2] tested circular carbon FRP (CFRP) confined STCC (CFRP-STCC) stub columns to investigate their eccentric compressive behaviour and presented *N*-*M* interaction relationship by a plastic stress distribution method. However, up to now, only a few parameters were studied to understand their effects of FRP wrap on the constitutive behaviour of confined concrete [28,31] and no research was reported about square FRP-STCCs. However, both constitutive behaviour and confinement mechanism are considered very important to the structural analysis of FRP-STCC structures. To develop a more reliable analysis constitutive model, more test studies on square FRP-STCC elements are needed to establish the stress-strain law of square FRP-STCCs.

The main objectives of the paper are to study the monotonic axial compressive behaviour of square CFRP-STCCs and to analyse the confinement mechanism of square steel tube and CFRP wrap in the confined concrete stub columns. Although CFRP materials are more expensive and have a small fracture strain and may cause potential galvanic corrosion issues, however, as a start of the study on the confined STCC elements, CFRP was first selected among commonly used FRP materials (i.e. CFRP, GFRP, aramid FRP, and basalt FRP). The main reasons are: (1) The elastic modulus of CFRP materials is close to that of steel materials, which meaning it is easier to work together with the steel tube, compared with the other FRP materials. (2) CFRP materials have a higher strength-weight ratio, which means it has a high potential to effectively improve the confinement of the inside concrete in STCC elements. (3) The basic research conclusions of CFRP-STCC are also applicable to those of the STCC confined by other FRP materials due to the inherent linear elastic response of FRP materials. Based on the experimental study, a calculation model was proposed to assess the axial bearing capacity of CFRP-STCC stub columns. The investigation mainly includes failure modes, load-deformation behaviour, the influence of main parameters (the number of layers of CFRP wrap, width-to-thickness ratio of steel tube, corner radius at sectional corner), and confining stress analysis of CFRP-STCCs.

2 Test investigation

2.1 Test specimens

In this study, total 23 specimens were prepared and tested, including 11 square CFRP-steel tube confined plain concrete (CFRP-STCC) stub columns, 3 square steel tube confined plain concrete (STCC) stub columns, 6 square CFRP-steel tube confined reinforced concrete (CFRP-STCRC) stub columns and 3 square steel tube confined reinforced concrete (STCRC) stub columns. The height-to-width ratio (H/B_0) of all specimens is 3.0. Fig. 2 gives the details of the test specimens. The volumetric ratios of the longitudinal reinforcement (4Φ12) and steel stirrup (Φ6@200) of confined RC specimens were 2.0% and 0.4%, respectively. The steel stirrups in the related specimens were only used to fix the longitudinal reinforcements, and the hoop confinement of them to the concrete core was ignored in the later analysis. In order to ensure that applied axial load was transferred uniformly to the internal longitudinal reinforcement in the specimens, both ends of each longitudinal rebar were welded to the bottom and top steel plates of each specimen (see Fig. 2b), respectively. In order to guarantee that the steel tube does not directly bear axial load in each specimen, a ring with a length of 10 mm was cut after casting from both ends of steel tube (40 mm from the ends), forming two girth gaps in each specimen shown in Fig.2. A wet lay-up process was used to conduct CFRP wrap to steel tubes in the specimens. Before CFRP was wrapped, the floating rust and impurities on the surface of the steel tubes were removed with a fine sandpaper and using an alcohol treatment. CFRP sheets with the same height as that of the steel tube were then uniformly and tightly wrapped on the outer surface of the steel tube with an epoxy adhesive. The overlapping length of CFRP sheets was 120 mm according to the Chinese Code (GB 50608-2010) [32], which was arranged to cover one of the welding seams of steel tube (seen Fig. 3). The details of each specimen are listed in Table.1. The studied corner radiuses of the steel tubes were 10 mm, 20 mm, 30 mm, as PC-D-2-2(10), PC-B-2-2 and PC-D-2-2(30) specimens listed in the table, respectively.

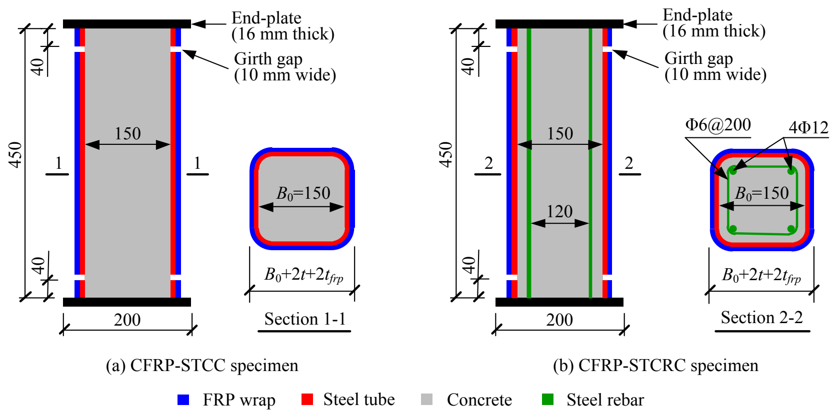

Fig. 2. Details of test specimens (Units in mm).

Table.1 Details of test specimens

Types	Specimen no.	Steel tube		CFRP		R /mm	Cross section
		t /mm	B/t	n	t_{frp} /mm		
Confined plain concrete (PC)	PC-A-1-0	1	152	0	0	20	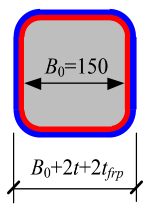
	PC-A-1-1	1	152	1	0.167	20	
	PC-A-1-2	1	152	2	0.334	20	
	PC-A-1-3	1	152	3	0.501	20	
	PC-B-2-0	2	77	0	0	20	
	PC-B-2-1	2	77	1	0.167	20	
	PC-B-2-2	2	77	2	0.334	20	
	PC-B-2-3	2	77	3	0.501	20	
	PC-C-3-0	3	52	0	0	20	
	PC-C-3-1	3	52	1	0.167	20	
	PC-C-3-2	3	52	2	0.334	20	
	PC-C-3-3	3	52	3	0.501	20	
	PC-D-2-2(10)	2	77	2	0.334	10	
	PC-D-2-2(30)	2	77	2	0.334	30	

Confined RC	RC-A-1-0	1	152	0	0	20	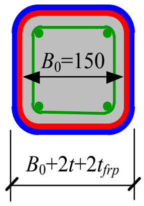
	RC-A-1-2	1	152	2	0.334	20	
	RC-A-1-3	1	152	3	0.501	20	
	RC-B-2-0	2	77	0	0	20	
	RC-B-2-2	2	77	2	0.334	20	
	RC-B-2-3	2	77	3	0.501	20	
	RC-C-3-0	3	52	0	0	20	
	RC-C-3-2	3	52	2	0.334	20	
	RC-C-3-3	3	52	3	0.501	20	

Note: B/t is the width-to-thickness ratio of steel tube; t and t_{frp} are the thickness of steel tube and CFRP wrap, respectively; n is the number of layers of CFRP; R is the corner radius of steel tube.

2.2 Material properties

The elastic modulus, the yield load, and the ultimate tensile strength of the used steel tubes were measured according to the Chinese Code, GB/T 228-2002 [33]. The test results are shown in Table 2. The longitudinal rebars were HRB 335 rebars with a diameter of 12 mm, a measured yield strength of 378 MPa and an ultimate tensile strength of 540 MPa. A standard commercial concrete with a maximum coarse aggregate size of 10.0 mm was used in all specimens which was supplied by a local company. Three cylinders of Ø150 × 300 mm were tested under axial compression to define the compressive strength of used concrete. The average compressive strength of unconfined concrete was 55.4 MPa. The related material properties of CFRP sheet (surface density: 300 g/m^2, provided by Toray Co., Ltd, Japan), and of epoxy adhesive (provided by Dalian Kaihua New Technology Engineering Co., Ltd, China), were provided by manufacturers and listed in Table 2. In order to avoid potential galvanic corrosion between CFRP wrap and steel tube in practical application, a thin insulating layer (i.e. Glass FRP) must be wrapped firstly before wrapping CFRP sheet on steel tube. However, the insulating layer was not applied in the study considering the test is short-term without such galvanic corrosion issue. Although the CFRP-STCC elements proposed in this paper are relative complex, consisting of steel rebars, concrete, steel tube, GFRP, CFRP, epoxy layers, and an additional protection layer, it is one of the ways to effectively solve the corrosion problem of steel tube. And if CFRP is replaced by GFRP in the elements, the additional insulating layer is not needed. Moreover, to resist the steel corrosion, similar technologies using FRP wrap on steel tube had already been applied in the structures with steel piles located in several harbours in China [31]. These projects preliminarily proved the effectiveness of the FRP wrap to resist steel corrosion of the structures. Therefore, as one of the treatments of durability and effective confinement methods, the proposed FRP-STCC elements present the potential of wide applications in practical projects to address the corrosion problem of steel tube and improve the structural performance of the elements. In addition, to simplify the analysis, the axial compressive behaviour contributed from the thin GFRP insulating layer can be omitted due to the layer can be very thin in the practical application of CFRP-STCC elements.

Table.2 Material properties of steel tube, CFRP sheet and epoxy adhesive

Materials	Nominal thickness /mm	Elastic modulus /GPa	Yield tensile strength /MPa	Ultimate tensile strength /MPa	Elongation /%
Steel #1	1.0	210	188	330	-
Steel #2	2.0	204	192	345	-
Steel #3	3.0	205	200	323	-
CFRP	0.167	245	-	4077	1.51
Epoxy	-	>2.5	-	>40	>1.80

2.3 Loading and measurement

The measurement and setup of the test are presented in Figs. 3 and 4. A monotonic axial compressive loading was applied on each specimen by a 5000 kN hydraulic compressive machine (see Fig. 4), which was controlled by vertical displacement with a rate of 0.5mm per minute referring to the literature [1]. The axial compressive load was measured by a load cell placed on the top of the specimens. Two linear variable displacement transducers (LVDTs) with a measurement range of 50 mm were arranged symmetrically on the diagonal direction of the test specimens to measure the vertical displacement of stub columns, as shown in Figs. 3 and 4. Twelve strain gauges with a gauge length of 20 mm were installed on CFRP wrap to measure the axial and hoop strains of CFRP wrap and steel tube at the mid-height of the test specimens, as shown in Fig. 3. Since CFRP wraps were well bonded to steel tubes with epoxy adhesive, the inner steel tube was considered to work together with the outer CFRP wrap without interfacial slippage. Therefore, the strains of the inner steel tube were assumed to be the same as those of the outer CFRP wrap. The strain and load information were collected synchronously at an acquisition frequency of 1.0 Hz.

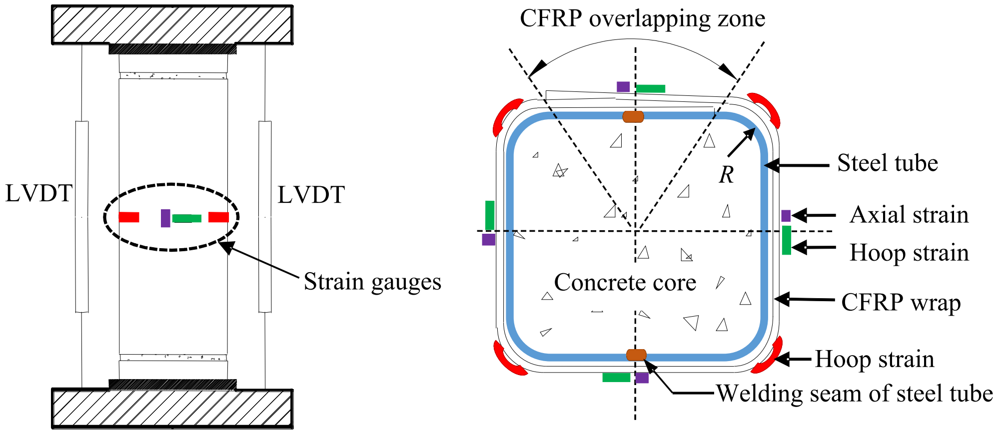

Fig. 3. Layout of LVDTs and strain gauges in the specimens.

Fig. 4. Test setup.

3 Test observations and analyses

3.1 Failure modes

The damage and failure modes of the steel tube confined concrete specimens and the CFRP-steel tube confined concrete specimens are shown in Fig. 5. In the steel tube confined concrete columns, the concrete cover at the ends of steel tube experienced sporadic crushing or spalling when approaching the peak loads of the columns. When the axial load dropped to around 70% of their peak load, the steel tube near the middle section suffered a significant outward local buckling. After removing the steel tubes, several obvious shear damages were observed in the steel tube confined plain concrete specimens, as shown in Fig. 5 (a), (b) and (c). On contrast, the shear failure was not pronounced in the steel tube confined RC specimens instead of evenly distributed cracks, as shown in Fig. 5 (f), (j) and (h), indicating that the installation of longitudinal reinforcements improved the axial compressive behaviour of steel tube confined concrete.

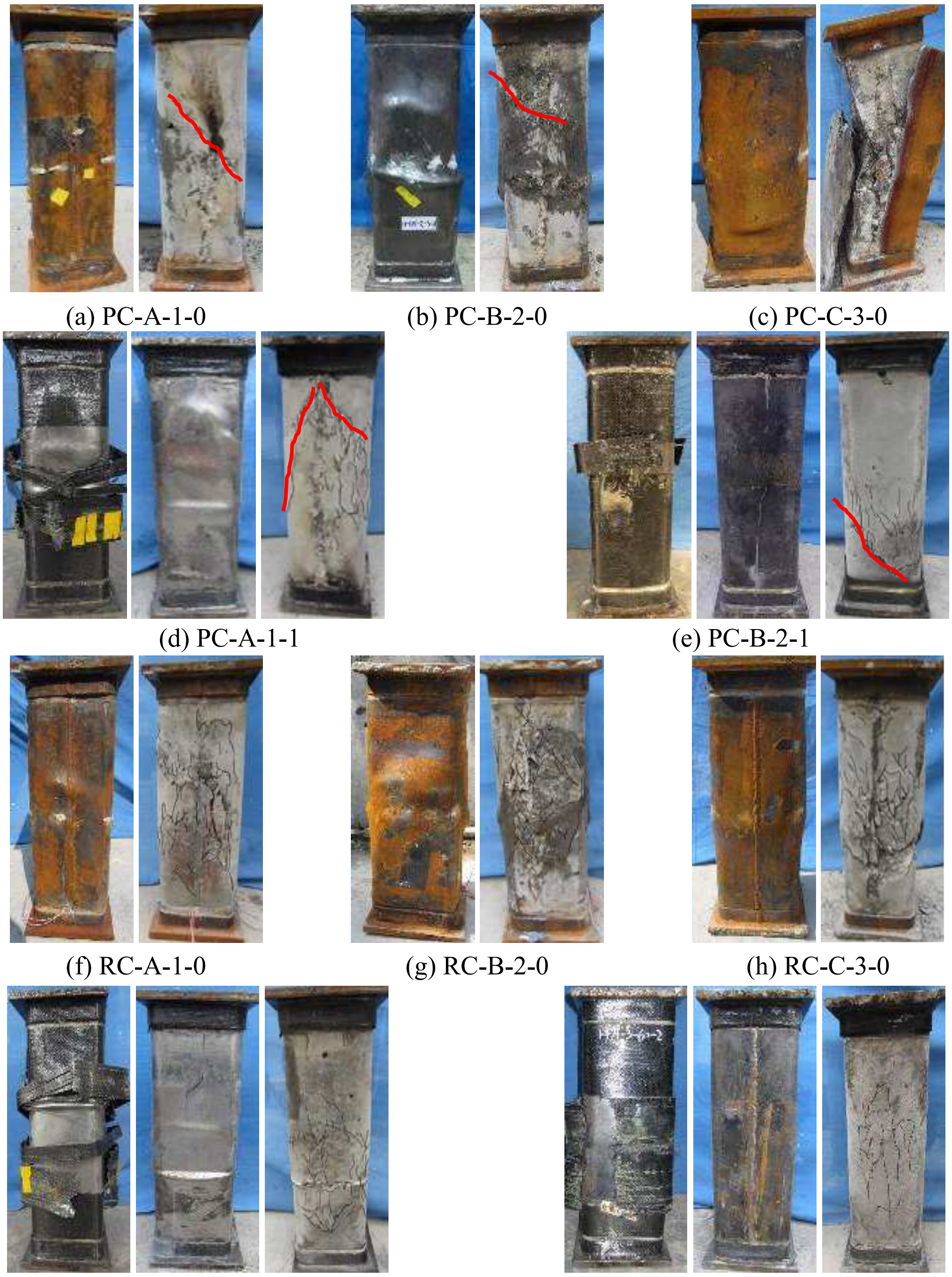

(a) PC-A-1-0 (b) PC-B-2-0 (c) PC-C-3-0

(d) PC-A-1-1 (e) PC-B-2-1

(f) RC-A-1-0 (g) RC-B-2-0 (h) RC-C-3-0

(i) RC-A-1-2 (j) RC-C-3-2

Fig. 5. Failure models of several representative confined concrete stub columns.

For the CFRP-steel confined concrete specimens, their ultimate failure was dominated by the hoop rupture of CFRP wrap (see Fig. 5 (d), (e), (i) and (j)). After the fracture of CFRP wrap, the local buckling of steel tube near specimens' mid-height section was observed and then the whole specimen failed. After removing the steel tubes, diagonal shear cracks still were observed in the surface of the concrete core in the specimens, shown in Fig. 5 (d) and (e). However, the shear failure was avoided in the CFRP-steel tube confined RC specimens (Fig. 5i and j), which confirms that the addition of longitudinal reinforcement can play a beneficial effect on the axial compressive behaviour of CFRP-steel tube confined concrete columns.

3.2 Axial load-strain behaviour

Figs. 6 and 7 depict the axial load-strain curves for several representative CFRP-steel tube confined plain concrete specimens. In this study, the nominal axial strain was calculated as a ratio of the axial shortening to the initial height of specimens, while the hoop strain was the average measured strain by four hoop strain gauges installed on the corners or middle sections.

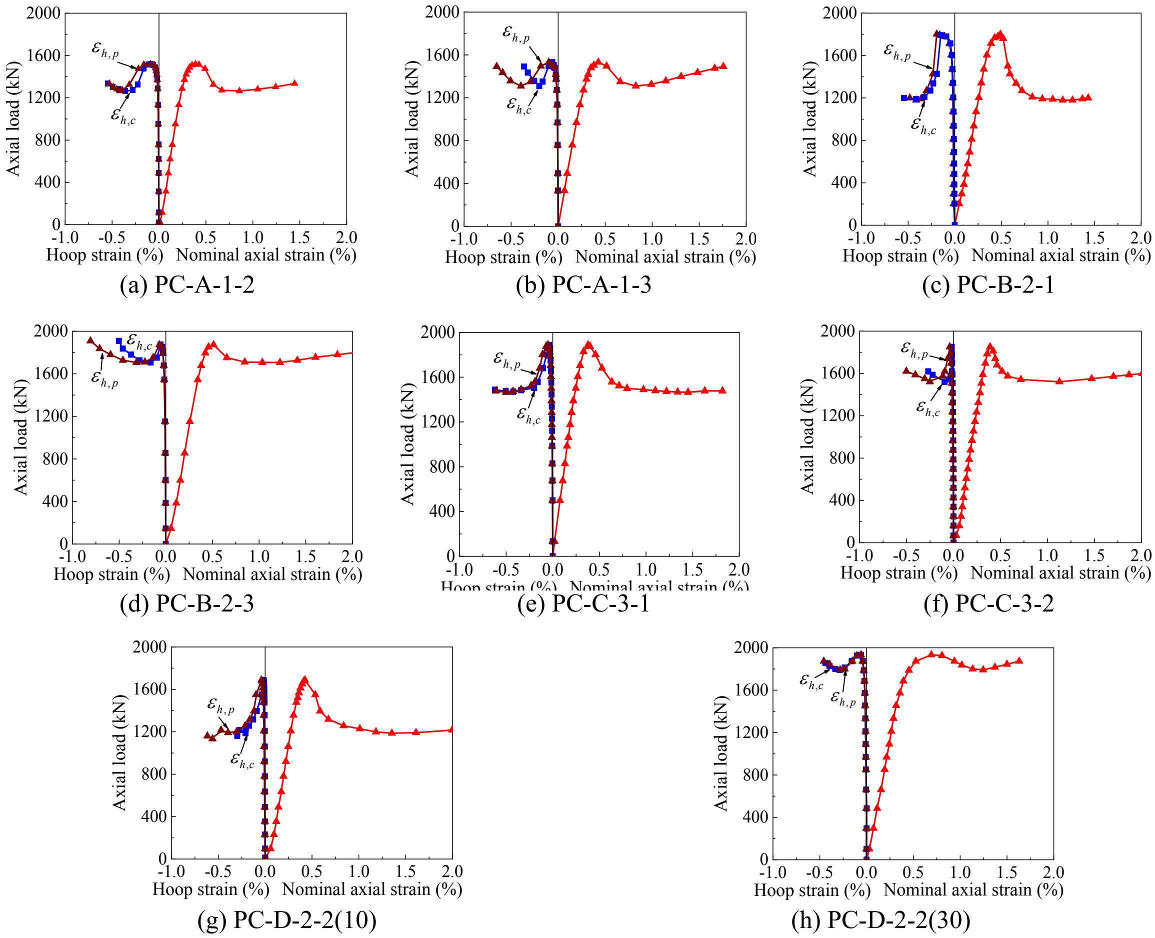

Fig. 6. Axial load-strain curves of confined plain concrete specimens.

Results show that all confined plain concrete and confined RC specimens deformed elastically at the early stage. The axial deformation increased approximately linearly, and its increasing rate was much greater than that of the lateral deformation. With the increasing of axial deformation, the lateral deformation at the corners ($\varepsilon_{h,c}$) was smaller than the deformation at the middle of steel tube side at the middle section ($\varepsilon_{h,p}$). This indicates that the concrete deformation at the corners of the steel tubes was restrained well while the other deformations at the middle section are not well confined. The bearing capacity of steel tube confined concrete specimens rapidly decreased after the specimens reached their peak loads, and the axial load tended to stabilize when the peak load was reduced to a certain load ranging from 50% to 90% of corresponding peak load.

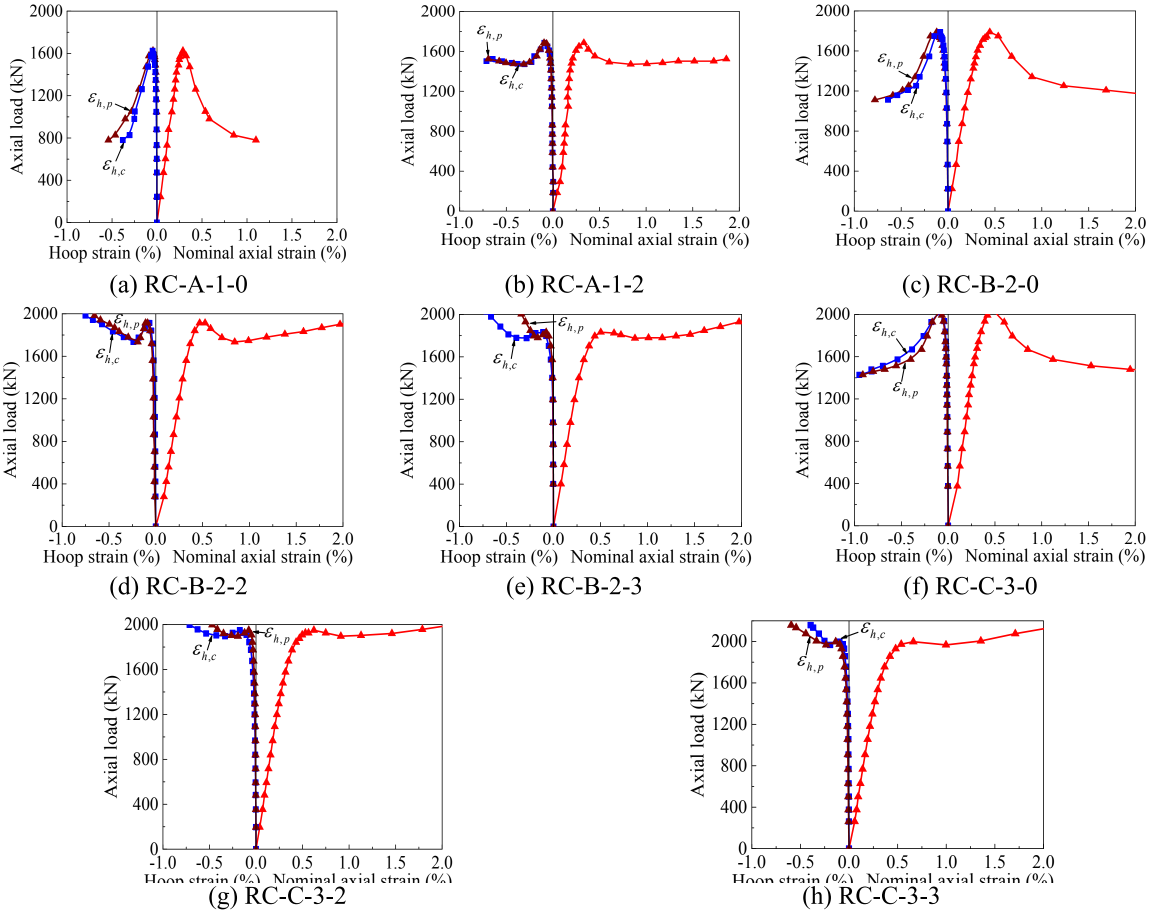

Fig. 7. Axial load-strain curves of confined reinforced concrete specimens.

For both CFRP-steel confined plain concrete and confined RC specimens, their load carrying capacity started to decrease after the specimens reached their first peak load. The lower the number of layers of CFRP was, the larger the decrease of the bearing capacity was. When the curves decreased to a certain extent, the hoop strain of the confined concrete started to increase and the curves began to slightly rise. The greater the number of layers of CFRP wrap used in the specimens, the higher the increase rate of the bearing capacity was. The softening phenomenon indicates that the confinement effectiveness of FRP-steel tube in square section concrete specimens was relatively weak. The softening phenomenon also occurred in CFRP-steel tube confined RC columns. However, the peak load of the curves in the second rising section was generally larger than that of the confined plain concrete specimens, e.g., PC-B-2-3 and RC-B-2-3 specimens. It shows that the deformability of confined concrete specimens was improved after reinforcing rebars were added to the columns. This improvement was more conducive to the development of the confinement effectiveness of the FRP-steel composite tube so that the load carrying capacity of the columns increased.

3.3 Stress-strain relationship of steel tube

The confinement of steel tube to concrete core can be understood by analysing the longitudinal and transverse stress of the steel tube. Referring to the literature [34], the stress of steel tube during loading was determined based on the hoop and axial strain in the middle of the specimen. This brings a better understanding of the confinement effectiveness of the steel tubes in the composite elements. Due to a thin-walled steel tube was used in this study, the force perpendicular to the wall of steel tubes is small and can be neglected. For this, the steel tube can be considered under the state of plane-stress [35]. Fig. 8 demonstrates the main calculation method of stress analysis of the steel tube at three stages. At the elastic stage, the stress-strain relationship was assumed to obey the Hooke's law. An elastic increment theory [34] was used to determine the stress of steel tube at the elastic-plastic stage (AB). The Von-Mises yield criterion and the Prandtl-Reuss flow rule were adopted to analyse the behaviour of steel tube at the plastic hardening stage (BC) [36]. In Fig. 8, σ_h and ε_h are the hoop stress and strain of steel tube, $\sigma_v$and ε_v are the axial stress and strain of steel tube, σ_z is the equivalent stress of steel tube, μ_s is Poisson's ratio of steel in the elastic stage, E_s^t and μ_{sp} are the tangent modulus and Poisson's ratio of the steel in the elastoplastic stage, $\sigma_h^{'}$, $\sigma_v^{'}$ and σ_{cp} are the hoop and axial deviatoric stress of steel and its mean stress, G is shear modulus of the steel, f_y and f_p are the steel yield strength and proportional limit ($0.8f_y$), ε_p and ε_y are the equivalent strain of steel corresponding to f_p and f_y, respectively. p, H' and Q are defined parameters for the calculation [34].

It should be noted that the transverse and axial strains used for the stress analysis of steel tubes are the strains at the middle of the mid-section of the steel tube. Fig. 9 shows the relationship between the axial load and the stress of steel tube developed in several specimens. The tensile stress was considered to have a negative sign in the stress analysis of steel tube. It was found that the axial stress increased more quickly than the hoop stress at the early stage, and the growth rate gradually increased with the increase of axial load. The yielding of steel tubes of the specimens was confirmed around their first peak loads. After that point, the hoop stress of the steel tubes increased slowly, but in some cases, a negative evolution was observed such as PC-B-2-1 and PC-D-2-2 (10). In these specimens, the axial load decreased sharply too. This leads to the fact that the confinement of steel tube to concrete core was effectively confined anymore after the significant expansion of concrete, which then affected the bearing capacity of the specimens. In the CFRP-steel tube confined concrete specimens, the hoop stress of the steel tube increased after the first peak load, and the load carrying capacity of the specimens decreased slowly or increased slightly such as Specimen RC-C-3-3. This implies that the FRP wrap can not only confine the concrete core, but can also confine the steel tube, which increases the confinement effect of the steel tube on concrete core.

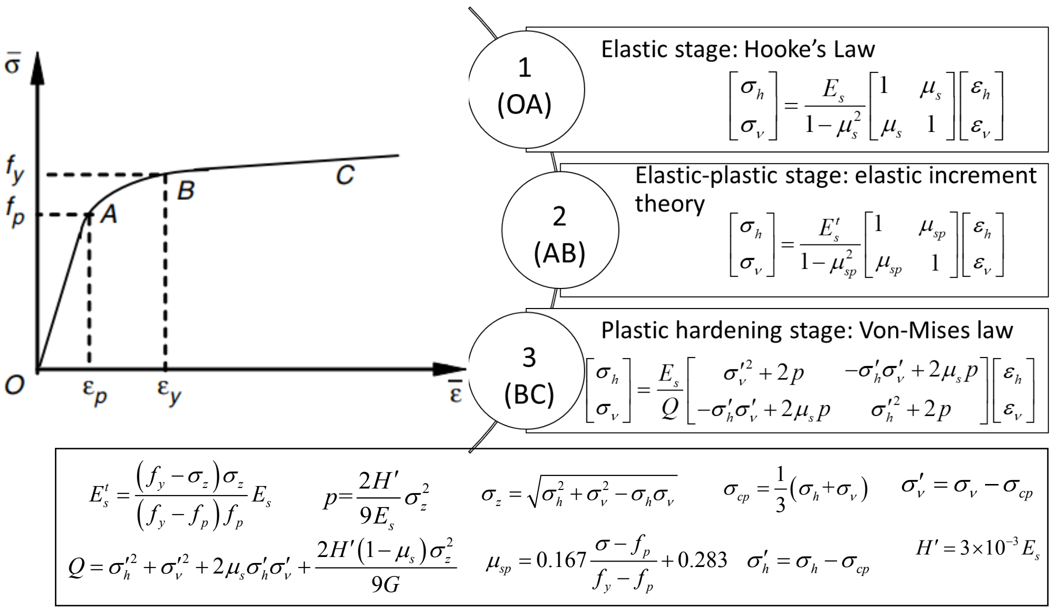

Fig. 8. Stress analysis of steel tube [34].

Besides, a similar test observation to that of the confined concrete specimens was confirmed in the confined RC specimens. The confinement effectiveness of the FRP-steel tube on the concrete core was stronger than those in the concrete specimens. For example, although the steel tube yielded in several specimens, their bearing capacity kept increasing (see RC-C-3-3). This implies that the CFRP-steel tube confined RC columns present better ductility and deformability compared to the confined plain concrete columns.

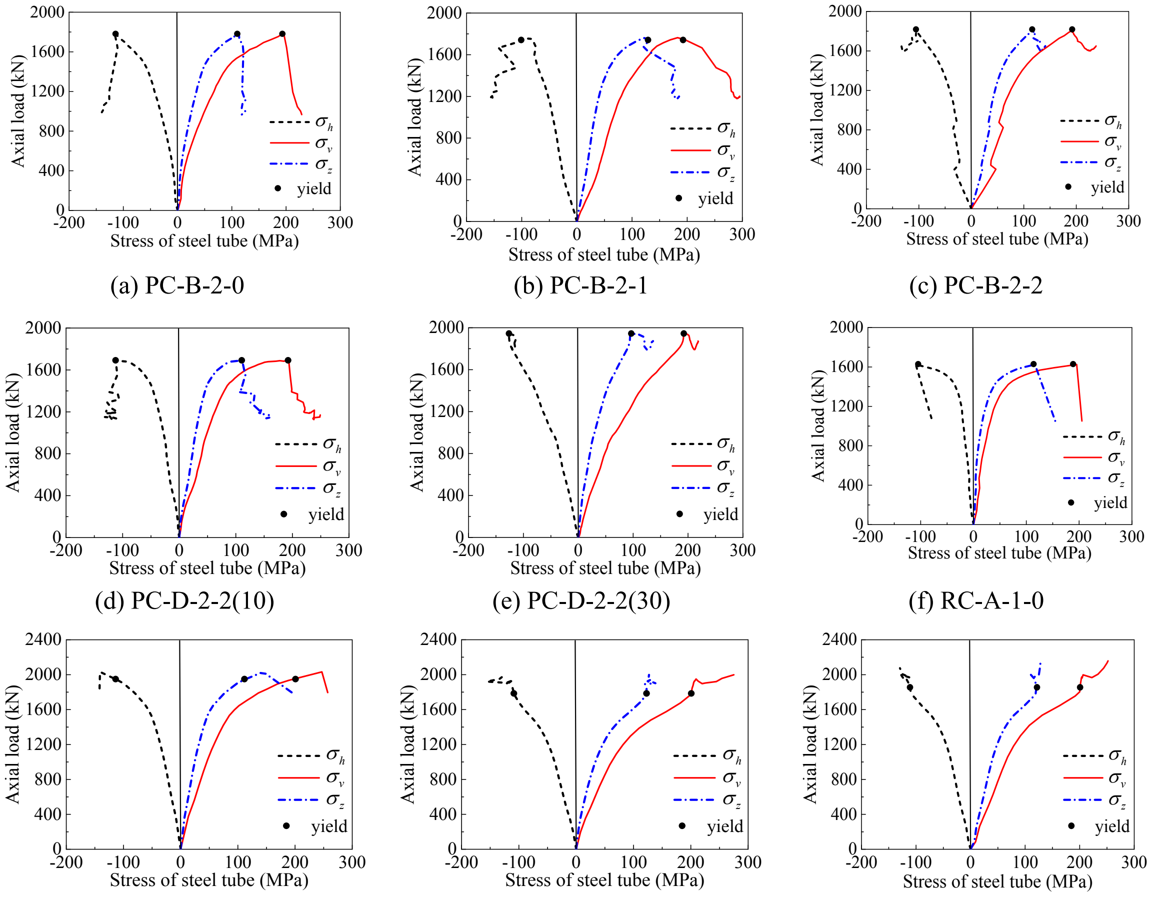

(a) PC-B-2-0 (b) PC-B-2-1 (c) PC-B-2-2

(d) PC-D-2-2(10) (e) PC-D-2-2(30) (f) RC-A-1-0

(g) RC-C-3-0 (h) RC-C-3-2 (i) RC-C-3-3

Fig. 9. Axial load-stress relationship of steel tube of representative specimens.

3.4 Stress-strain responses of confined concrete

Appling the stress analysis of steel tube, the axial load resisted by steel tube can be discussed. In addition, the main fibres of CFRP wrap are only oriented in the hoop direction, so that the stiffness of the CFRP wrap in the direction perpendicular to the hoop direction is very small and can be ignored. When the axial stiffness of CFRP wrap is ignored, the load supported by concrete core can be calculated as the total load of the specimens deducted the load resisted by steel tube. Assuming the compressive stress on the entire section of concrete core is uniformly distributed, the compressive load of confined concrete can be calculated by dividing the deducted load by its cross-sectional area. Moreover, for confined RC specimens, the axial bearing contribution of the longitudinal reinforcement should be deducted from the load resisted by whole column. In summary, the axial stress of confined concrete can be obtained by,

$$\sigma_c = \begin{cases} \dfrac{N - \sigma_v A_s}{A_c} & \text{for confined plain concrete} \\ \dfrac{N - \sigma_v A_s - f_a A_a}{A_c} & \text{for confined reinforced concrete} \end{cases} \tag{1}$$

where σ_c is the axial stress of confined concrete; N is the axial load resisted by whole column; σ_v is the axial stress of steel tube; f_a is the yield strength of longitudinal reinforcement in the columns; A_s, A_a and A_c are the cross-sectional areas of the steel tube, the longitudinal reinforcement and the concrete core, respectively. Besides, the axial deformation of the confined concrete is believed to be identical to the nominal axial strain of the specimens. Table.3 lists a summary on the calculated results of the axial stress and measured strain of the concrete cores in the specimens, while Fig. 10 shows the stress-strain curves of the confined concrete.

Results plotted in Fig. 10 demonstrate that the initial elastic moduli of the confined plain concrete and RC are basically identical when compared within the same group. The first peak stress of the CFRP-steel tube confined plain concrete specimens in Groups PC-A and PC-B (or Groups RC-A and RC-B for confined RC specimens) were larger than those of the STCC specimens. The difference among the CFRP-steel tube confined concrete or RC specimens was small, especially in Groups PC-C and RC-C. This is explained by the fact that the *B*/*t* ratio of steel tube in Group A is large (*B*/*t* = 152) indicating that the confining stress of the steel tubes was much smaller than others for it is prone to be buckling failure. This also is the reason why the relatively weak confinement to suppress the expansion deformation of the concrete cores in the specimens. When FRP wrap was used, the wrap can not only restrain the lateral dilation of concrete core but also suppress the local buckling deformation of steel tube, so that steel tube can continue to exert its confinement effect.

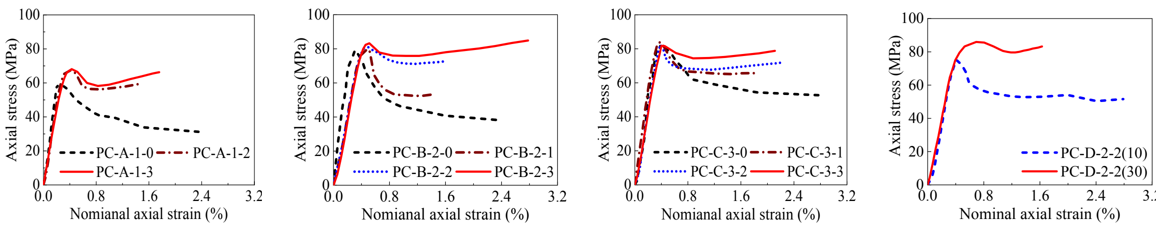

(a) PC-A-1 (b) PC-B-2 (c) PC-C-3 (d) PC-D-2

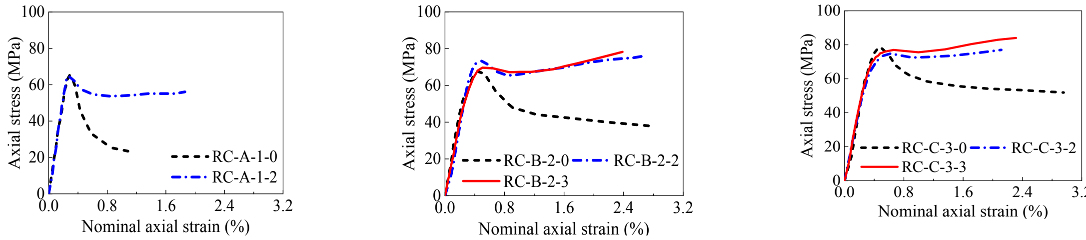

(d) RC-A-1 (e) RC-B-2 (f) RC-C-3

Fig. 10. Axial stress-strain curves of confined concrete.

Table 3. Summary of axial stress and axial strain of confined concrete.

Groups	Specimens	f_{cc1} /MPa	ε_{cc1} /%	f_{cc2} /MPa	ε_{cc2} /%
PC-A	PC-A-1-0	58.84	0.207	—	—
	PC-A-1-2	67.50	0.389	59.32	1.45
	PC-A-1-3	68.11	0.428	66.30	1.76
PC-B	PC-B-2-0	79.23	0.313	—	—
	PC-B-2-1	79.89	0.490	53.33	1.43
	PC-B-2-2	80.90	0.498	72.79	1.62
	PC-B-2-3	83.24	0.512	84.86	2.78
PC-C	PC-C-3-0	82.14	0.418	—	—
	PC-C-3-1	83.86	0.378	65.67	1.82
	PC-C-3-2	82.28	0.388	72.02	2.24
	PC-C-3-3	81.71	0.402	78.80	2.12
PC-D	PC-D-2-2 (10)	75.03	0.425	51.56	2.78
	PC-D-2-2 (30)	85.94	0.692	83.24	1.63
RC-A	RC-A-1-0	63.95	0.274	—	—
	RC-A-1-2	64.87	0.300	50.86	1.86
RC-B	RC-B-2-0	67.80	0.445	—	—
	RC-B-2-2	73.24	0.526	76.28	2.72
	RC-B-2-3	69.67	0.503	78.24	2.39
RC-C	RC-C-3-0	78.47	0.489	—	—
	RC-C-3-2	74.84	0.622	76.98	2.12
	RC-C-3-3	76.98	0.662	84.02	2.31

Note: f_{cc1} and ε_{cc1} are the first peak stress and corresponding nominal axial strain of confined concrete; f_{cc2} and ε_{cc2} are the ultimate stress and corresponding nominal axial strain of confined concrete at the rupture of FRP wrap.

In the confined plain concrete and RC specimens, following the first peak axial stress, the effective confining stresses of the steel tube and FRP wrap in the square section are relatively small. Similar to previous research, the confinement is effective only in a limited confinement area in square concrete. It cannot prevent the expansion deformation of concrete in the non-effective confinement area. This was the reason why the stress-strain curves of the concrete exhibited different degrees of softening. The softening segment was smaller as the number of CFRP layers increased, and the stress-strain curves of confined concrete after this stage increased with varying degrees. This indicates that the lateral expansion deformation of the concrete core increased and the confining stress of CFRP wrap increased, leading to an increase in confining stress to the concrete core. The axial stress of the confined concrete increased until the hoop rupture of CFRP wrap. The slope of the secondary ascending branch of the axial stress-strain curves increased with the number of layers of CFRP. Besides, the corner radius of the steel tube has a significant influence on the stress-strain curves of confined concrete, as shown in Fig. 10 (d). Results show that the strength and ductility of confined concrete corresponding to a steel tube with a corner radius of 30 mm is significantly better than that of the specimen with a corner radius of 10 mm.

In addition, it is worth mentioning that the size effect also is an important affecting factor of the composite confined columns especially for square columns. The hoop strain of CFRP wrap is non-uniformly distributed along the circumferential direction. The hoop strain of CFRP wrap at the corners varies with the sectional size of square columns, leading to a considerable influence on the compressive behaviour of confined concrete. To the best of the authors' knowledge, the size effect in square FRP-steel tube confined plain concrete or RC columns has not been understood well. However, the study conducted by Wang et al. [37] on square FRP-confined RC columns can provide a significant reference to this issue. The experimental results [37] revealed that the compressive strength of square FRP-confined concrete decreased with cross-section size, while ultimate axial strain was influenced little by section size. Therefore, the size effect also may have an important impact on the axial compressive behaviour of square FRP-STCC elements, which deserves further concerns in the future.

3.5. Effects of test parameters

(1) Effect of the number of CFRP layers

Fig. 11 depicts the effect of the number of CFRP layers on the axial load-strain behaviour of steel tube confined concrete specimens and CFRP-steel tube confined concrete specimens, where the lateral strain is the measured strain at the corners of the specimens. Results show that the number of CFRP layers affects the first peak loads and corresponding axial strain. When the number of CFRP layers increased, the degree of post-peak softening of the specimens decreased significantly. After the first peak load, the curves of the CFRP-steel tube confined concrete specimens were much smoother than those of the steel tube confined concrete specimens. The more CFRP layers were used, the more gradual the curves exhibited and the higher the ultimate axial deformation of the specimens was. A significant increase was confirmed in the axial load-strain responses of the specimens with 3-ply FRP wrap after their softening stage, which is demonstrated by the fact that the bearing capacities of the specimens even exceeded their first peak loads in some cases. This indicates that the CFRP wrap can work with steel tube together to provide an effective confinement to concrete core, where the steel tube can effectively prevent the local and sharp damage of FRP wrap while the FRP can confine the steel tube at large hoop deformations.

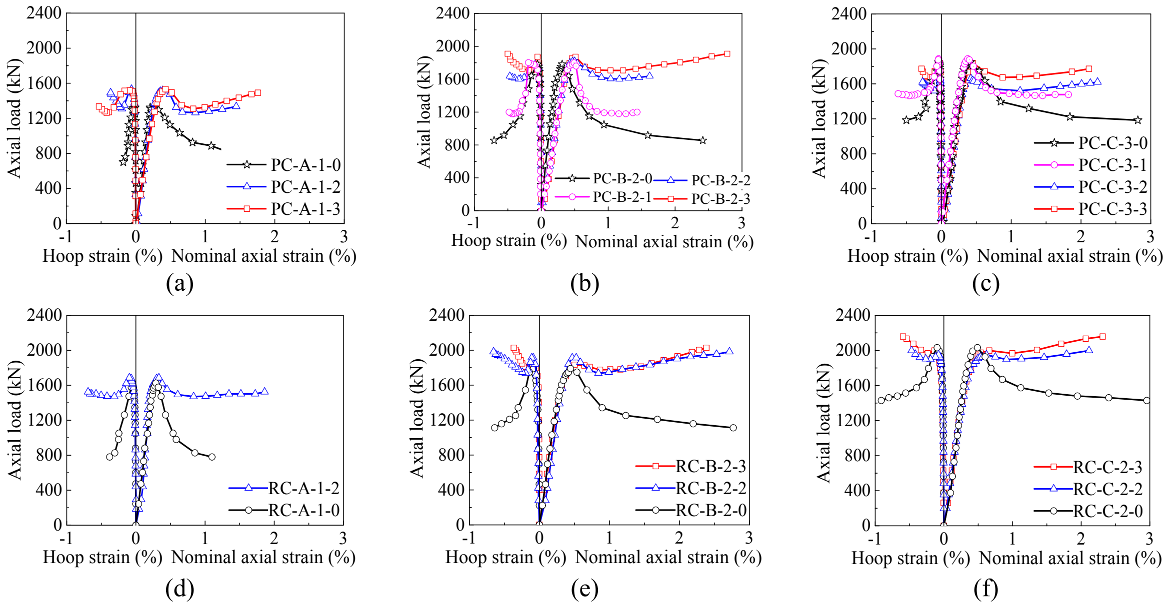

Fig. 11. Effect of the number of CFRP layers.

For the CFRP-steel tube confined RC specimens, the elastic behaviour and first peak load of the specimens are not significantly affected by the number of CFRP layers. The first peak loads were slightly larger than those of steel tube confined specimens. After first peak load, the axial load-strain curves of the CFRP-steel tube confined RC specimens continued to rise until the rupture of CFRP wrap. The ultimate bearing capacities of the CFRP-steel tube confined RC specimens with 3-ply FRP wrap corresponding to the rupture of FRP wrap were larger than their first peak loads. This means that with the increase of the number of CFRP layers, the co-confinement effectiveness of CFRP-steel tube to the square concrete core is significantly enhanced.

(2) Effect of the width-to-thickness (*B*/*t*) ratio of steel tubes

As shown in Fig. 12, the specimens with higher *B*/*t* ratio present smaller bearing capacities. Compared to the load capacity of the specimens using a *B*/*t* ratio of 152.0, the first peak loads of both the specimens with *B*/*t* ratios of 52.0 and 77.0 were higher. This means that the *B*/*t* ratio of the steel tube has a significant influence on the bearing capacity of the CFRP-steel tube confined concrete specimens. This is similar to the cases of the steel tube confined concrete elements. Besides, the smaller the B/t ratio was, the higher the load carrying capacity and ductility of the stub columns were. A similar result was found in the CFRP-steel tube confined RC specimens, but it seems that the B/t ratio has a slightly stronger influence on the first peak loads and on the ductility of the specimens.

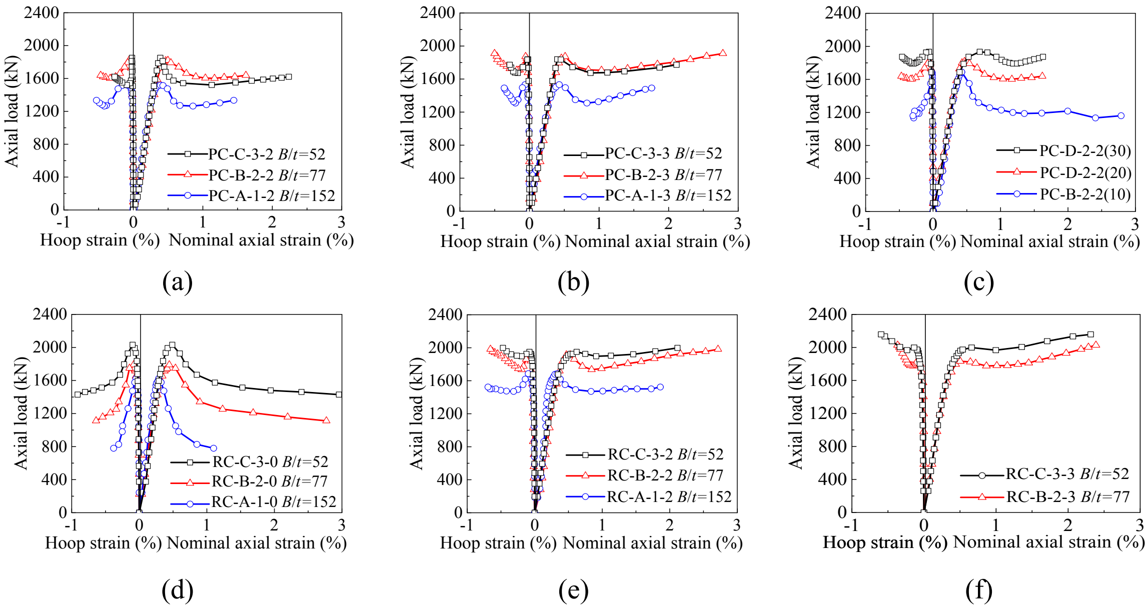

Fig. 12. Effect of width-to-thickness on axial load-strain curves at different FRP layers.

(3) Effect of corner radius at sectional corners

The effects of three levels of the corner radius of steel tube were experimentally study, i.e., 10 mm, 20 mm and 30 mm, respectively, as shown in Fig. 11 (c). The results show that the ultimate load of the specimens increases significantly with the increase of the corner radius. The softening behaviour of the curves after the first peak load was significantly reduced and slowed down as the radius increases. This presents the potential to improve the mechanical properties of square sectional confined plain concrete or RC columns by properly increasing the corner radius of column section. This is explained by the fact that more concrete core can be effectively confined in the columns, which is illustrated later in the study.

4. Discussion on confinement mechanism

4.1 Effective confinement of steel tube and FRP in confined square section

With reference to the cases in traditional square stirrup confined concrete, the effective confinement mechanism of either steel tube confined concrete or FRP-steel tube confined concrete is presented in Fig. 13. In these sections, only the concrete in the area enclosed by four parabola lines with initial tangent lines 45º from the corresponding sides of the section (see Fig. 13 (a)) can be effectively confined. This is a significant difference compared to the cases in circular confined- plain concrete or RC. Pham and Hadi [38] proposed a confinement mechanism of the concrete in confined square columns, which is shown in Figs. 13 (b) and (c). The confining stress at the corners is much larger than that at the four sides since the curvature radius of sectional sides is much greater than that of the corners. The confining stress f_r at the corners is given as

$$f_r = \frac{\sigma_{h,j}}{R} \tag{2}$$

where $\sigma_{h,j}$ is the hoop stress of a confining jacket at the corners; R is the corner radius.

According to Section 3.3, the confining stress provided by the steel tube $f_{r,s}$ is expressed as

$$f_{r,s} = \frac{\sigma_h}{R} \tag{3}$$

where σ_h is the hoop stress of steel tube at the corners.

Therefore, according to Fig. 13 (c), the confining stress of FRP wrap $f_{r,frp}$ is given as

$$f_{r,frp} = \frac{\sigma_{h,frp}}{R+t} = \frac{E_{frp}\varepsilon_{f,c}t_{frp}}{R+t} \tag{4}$$

where $\sigma_{h,frp}$ and $\varepsilon_{f,c}$ are the hoop stress and hoop strain of the FRP wrap at corners, respectively; E_{frp} and t_{frp} are the Young's modulus and thickness of FRP wrap, respectively.

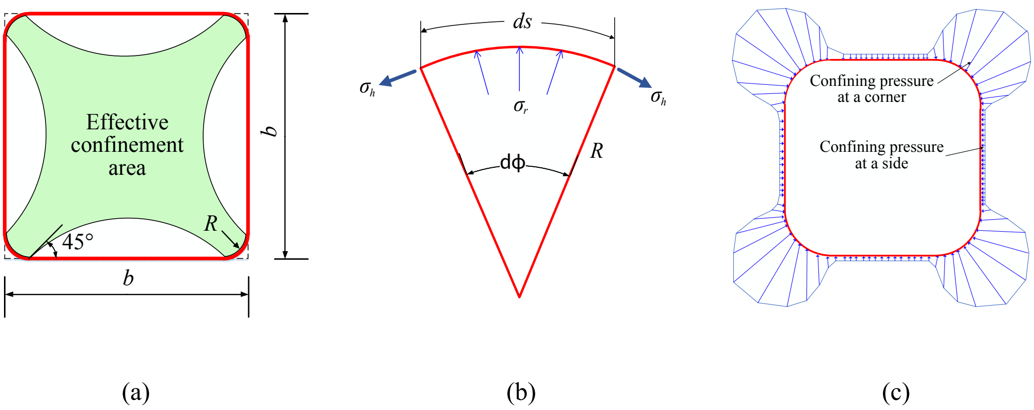

Fig. 13. The confinement of square confined concretes: (a) effective confining area of confined concrete; (b) stress distribution; and (c) confinement mechanism of FRP confined concrete [38].

Fig. 14 shows the evolution of the confining pressure of the steel tube and the CFRP wrap in the specimens, as well as the total confining pressure with the increasing nominal axial strain of the stub columns. Results show that the confining pressure of the steel tube increases rapidly at the initial stage of loading, and then increases slowly or almost remains constant during the later period. This indicates that the confining pressure of steel tube to the concrete core is limited after the yielding of the steel tube. On the other hand, the confining pressure provided by CFRP wrap was not high at the initial loading. Due to the increase of the lateral deformation of the steel tube, the FRP wrap started to provide a higher confining stress, for example, from an axial strain of 0.004 to 0.006. After that, the confining pressure of the CFRP wrap increased until the rupture of the FRP wrap. No obvious difference was found between the CFRP-steel tube confined plain concrete and RC specimens.

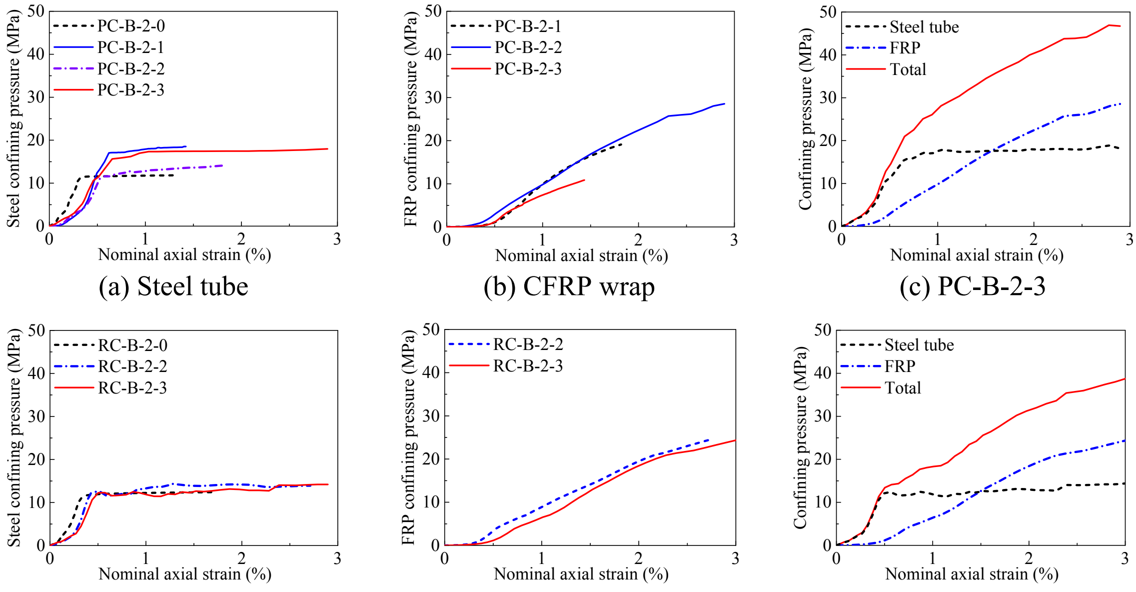

(a) Steel tube (b) CFRP wrap (c) PC-B-2-3

(d) Steel tube (e) CFRP wrap (f) RC-B-2-3

Fig. 14. Confining pressure provided by the steel tube and the CFRP wrap.

4.2 Confinement mechanism of square FRP-steel tube confined concrete/reinforced concrete

Based on the above analysis, Fig. 15 shows an ideal evolution of various confining pressures in FRP-steel tube confined plain concrete and RC columns, which explains the confinement mechanism of the composite tube to concrete core. The evolution of the confining pressure provided by steel tube and FRP wrap in the composite columns is similar to that observed in FRP-confined CFT specimens reported by Hu *et al.* [1]. However, the confinement mechanism of the specimens still is different from that in FRP-confined CFT specimens for the steel tube does not directly carry the axial load.

According to Fig. 15, the confinement actions in FRP-steel tube confined plain concrete and RC columns can be divided into three stages as follows,

(1) 1st stage – steel tube confinement stage

In this stage, the confining pressure of the concrete core comes mostly from the confinement of steel tube, while the confinement from FRP wrap can be nearly neglected. This is because the test specimens are only subjected to a small axial compression load, resulting in a very small lateral expansion in the concrete core at this stage. There are few obvious differences between the confined plain concrete and the confined RC columns as the stirrups were limited and only to erect the longitudinal reinforcements in the study. Therefore, it is believed that the stirrups only provide a quite small confinement to the concrete core. The small lateral deformation induced by a small axial strain in the concrete core does not need the confinement action of FRP wrap. Therefore, if the potential deformation of the confined plain concrete or RC columns remains at this level, the additional FRP confinement is not necessary from the point of view of the mechanical performance of the elements.

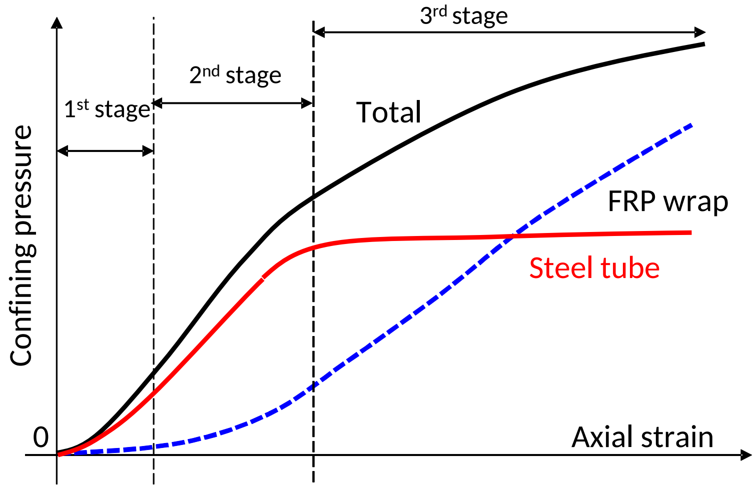

Fig. 15. Ideal confinement in FRP-steel tube confined concrete columns.

(2) 2nd stage – FRP-steel tube co-confinement stage

The second stage can be considered as a co-confinement stage consisting of both the confining pressures from steel tube and FRP wrap. However, as shown in Fig. 15, the two types of confining pressures increase at different rates depending primarily on their hoop stiffness. This stage is similar to the case in FRP-confined CFT columns [1]. The total confining pressure increases rapidly in this stage, as the lateral deformation of concrete core starts to rapidly increase. Based on the experimental investigation in the present study, the second stage can be delimited to a nominal axial strain of around

0.006. The FRP and steel tube work together in this stage and delay their respective fracture or local buckling due to the contribution of each partner.

(3) 3rd stage – FRP-dominated confinement increasing stage

The third stage of the confinement of FRP-steel tube confined concrete is dominated by FRP confinement. In this stage, the increasing total confining pressure to inner concrete comes mainly from the increasing confinement of FRP wrap, as the confinement of the steel tube keep almost a constant level after its yielding. The high strength feature of FRP materials becomes apparent at this stage. At the same time, the behaviour of the FRP material itself still is highly elastic, and the confining pressure of the FRP wrap can keep a similar increasing rate to that of the second stage. Therefore, at this stage, the increasing rate of the total confining pressure of onfined concrete or RC columns at this stage becomes smaller than that of the second stage, which is similar to the previous research results of FRP-confined CFT columns [1].

5. Proposal for predicating axial bearing capacity of composite square stub columns

Referring to previous research [39, 40], the superposition principle was used to predict the axial bearing capacity of CFRP-steel tube confined plain concrete or RC stub columns (N_u), which is given as

$$N_u = f_{CFS} A_c + f_a A_a \tag{5}$$

where A_c and A_a are the cross-sectional areas of concrete core and longitudinal reinforcement, respectively; f_a is the yield strength of longitudinal reinforcement; and f_{CFS} is the compressive strength of CFRP-steel tube confined concrete.

Based on the test results reported in this paper, a superposition calculation method is applied to predict the axial bearing capacity of CFRP-steel tube confined plain concrete or RC stub columns, consisting of the contribution of steel tube and FRP wrap. The discussion on the steel tube, FRP and FRP-steel tube confined concrete is presented in the following sections.

(1) For steel tube confined concrete

According to the literature, the calculation model for steel stirrup-confined concrete strength f_{cc} proposed by Mander et al. [41] is given as

$$f_{cc} = f_{co}\left(1 + 2.254\sqrt{1 + \frac{7.94 f_r}{f_{co}}} - 2\frac{f_r}{f_{co}} - 2.254\right) \tag{6}$$

where f_{co} is the compressive strength of unconfined concrete, and f_r is the confining pressure provided by steel stirrups.

Referring to this model, the ultimate compressive strength of steel tube confined concrete (f_{CS}) is given as

$$f_{CS} = f_{co}\left(1 + 2.254\sqrt{1 + \frac{7.94 f_{r,s}}{f_{co}}} - 2\frac{f_{r,s}}{f_{co}} - 2.254\right) \tag{7}$$

where $f_{r,s}$ is the confining pressure provided by steel tube calculated based on a static equilibrium, which is given as

$$f_{r,s} = \frac{2\sigma_h t}{B - 2t} \tag{8}$$

$$\sigma_h = \beta f_y \tag{9}$$

where σ_h is the hoop stress of the steel tube corresponding to the peak load of confined concrete columns; B and t are the width and thickness of square steel tube, respectively; β is a reduction factor related to the yielding strength of steel f_y. Previous studies [39, 40] proposed a similar prediction model and suggested the factor β, which is influenced by the width-thickness ratio of steel tube ranging from 50 to 100. However, based on the test results in this study, an average value of 0.62 was taken for the simplification of the calculations.

(2) For FRP-confined concrete

Based on the model proposed by Lam and Teng [42], the ultimate strength of square FRP-confined concrete (f_{cF}) is suggested as

$$f_{CF} = f_{co}\left[1 + k_1 k_{s1}\left(\frac{f_{r,FRP}}{f_{co}}\right)\right] \tag{10}$$

In this equation, $f_{r,FRP}$ is the confining pressure provided by FRP wrap to an equivalent circular column [42], and the confinement effectiveness coefficient k_1 = 3.3, same as defined in Lam and Teng model [43] for uniformly confined concrete. Referring to Ref. [42], k_{s1} is defined as a shape factor calculated as

$$k_{s1} = 1 - \frac{2}{3}\frac{(B_0 - 2R)^2}{B_0^2 - (4-\pi)R^2} \tag{11}$$

where R is the corner radius of inner concrete. Referring to the literature [38, 44], the confinement effectiveness is reduced at the corner of concrete [45]. Therefore, the confining pressure of FRP to concrete ($f_{r,FRP}$) is expressed as

$$f_{r,FRP} = \frac{n\, t_{frp}\, k_c\, k_r\, E_{frp}\, \varepsilon_{h,rup}}{D} \tag{12}$$

where n is the number of layers of FRP wrap; D is an equivalent diameter which is taken as $\sqrt{2}B_0$ in this paper; t_{frp} is the thickness of FRP wrap; E_{frp} and $\varepsilon_{h,rup}$ are the elastic modulus and the hoop rupture strain of FRP wrap. Referring to the method introduced by Hadi et al. [44], a corner-effect coefficient k_c was introduced to reduce the stronger confining stress at the corner. The factor was defined as the ratio of the sum of the corner length to the sectional perimeter and given as

$$k_c = \frac{\pi R}{2B_0 - (4-\pi)R} \tag{13}$$

Besides, to consider the effect of the large curvature of the corners on FRP wrap leading to a stress concentration of the FRP wrap, the reduction factor k_r is introduced. Based on the literature [45], the factor is taken as

$$k_r = \left(1 - 0.2121 \times \frac{\sqrt{2}}{2}\right)\frac{2R}{B_0} + 0.2121 \times \frac{\sqrt{2}}{2} \tag{14}$$

The FRP efficiency factor (k_ε) is defined as the ratio of recorded hoop rupture strain of FRP ($\varepsilon_{h,rup}$) to the ultimate tensile strain of FRP obtained from flat coupon tests (ε_{frp}), which is shown in Eq. (15) and taken as 0.33 based on the test results of the study.

$$k_\varepsilon = \varepsilon_{h,rup}/\varepsilon_{frp} \tag{15}$$

(3) For FRP-steel tube confined concrete

The steel tube confinement is generally regarded as an active confinement because the confining pressure provided by steel tube almost remains constant after the yielding of steel tube. On contrast, the FRP confinement is generally considered as a passive confinement because the confining pressure provided by FRP wrap increases continuously with the lateral dilation of concrete. Therefore, the FRP-steel composite confinement might be a confinement type between active confinement and passive confinement. Theoretically, the steel tube-FRP composite confinement in the study can be regarded as one integral confinement since the two confining materials are well bonded based on the tests in the study. However, up to now the theoretical model of FRP-steel composite confined concrete is not researched well. In the present study, a simplified superposition calculation method was used based on the understanding of steel-confined concrete and FRP-confined concrete. As a start, the simplified method is relatively rough but easier to be understood by structural engineers.

Based on the superposition principle, the ultimate strength of square FRP-steel tube confined concretes can be calculated as a total strength consisting of the contribution components of FRP wrap and steel tube, which is given as

$$f_{CFS} = f_{co}\left[1 + \left(2.254\sqrt{1 + \frac{7.94 f_{r,s}}{f_{co}}} - 2\frac{f_{r,s}}{f_{co}} - 2.254\right) + k_1 k_{s1}\left(\frac{f_{r,FRP}}{f_{co}}\right)\right] \tag{16}$$

Taking Eqs. (7) and (16) into Eq. (5), the axial bearing capacities of steel tube confined concrete stub columns and FRP-steel tube confined concrete stub columns are expressed as

$$N_u = \begin{cases} f_{co}\left(1 + 2.254\sqrt{1 + \frac{7.94 f_{r,s}}{f_{co}}} - 2\frac{f_{r,s}}{f_{co}} - 2.254\right)A_c + f_a A_a \\ f_{co}\left[1 + \left(2.254\sqrt{1 + \frac{7.94 f_{r,s}}{f_{co}}} - 2\frac{f_{r,s}}{f_{co}} - 2.254\right) + k_1 k_{s1}\left(\frac{f_{r,FRP}}{f_{co}}\right)\right]A_c + f_a A_a \end{cases} \tag{17}$$

Fig. 16 compares the prediction results of proposed model with the experimental results in this study. Regardless of the confinement types, the proposed model evaluates the ultimate bearing capacities of these confined plain concrete and RC columns with a great agreement.

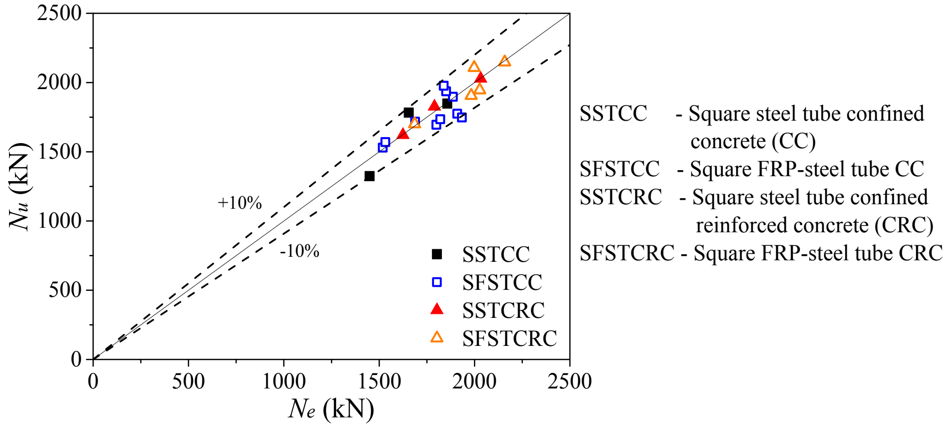

Fig. 16. Comparisons between calculated and experimental results.

In addition to the axial bearing capacity, ultimate axial strain of composite stub columns is a very important parameter. For square STCC specimens, as shown in Table 3, the strain capacity increases with the thickness of steel tube because a thicker steel tube usually can provide a larger confinement to concrete core. Moreover, the installation of longitudinal reinforcements also can improve strain capacity. For square FRP-STCC specimens, the strain capacity generally increases with the thickness of steel tube, the number of layers of FRP wrap and the installation of longitudinal reinforcements. Therefore, the confinements from steel tube and FRP wrap as well as the advantageous effects of longitudinal reinforcement should be considered when predicting the strain capacities of square STCC stub columns and square FRP-STCC columns, which is expected to be studied in the future.

6. Concluding remarks

This paper presented an experimental study to understand the monotonic axial compressive behaviour and confinement mechanism of square CFRP-steel tube confined concretes. The confinement from steel tube and CFRP wrap enhances the ultimate strength and ductility of core concrete. CFRP wrapping effectively constrains the deformation of steel tube, which delays its outward local buckling and constrains the continuous dilation of core concrete at the stage of large deformation. Based on this study, the following conclusions can be drawn:

1. The CFRP-steel tube confinement is highly effective in improving the bearing capacity and ductility of concrete columns, especially for plain concrete. The number of layers of CFRP wrap has a significant effect on the failure of the confined reinforced concrete columns. The width-to-thickness ratio of the steel tube is also a key factor affecting the axial bearing capacity of confined concrete columns.

2. The post-peak softening phenomenon of square confined concretes was observed in the specimens. However, the softening degree of the columns was improved by using a thicker CFRP wrap. The effect of the CFRP wrap is more pronounced for the CFRP-steel tube confined concrete columns with a larger width-to-thickness ratio of steel tube.

3. Through a detailed stress analysis, the stress-strain curves of the concrete core confined by composite action of steel tube and CFRP wrap were provided. The mechanical properties of the concrete core was greatly improved by the composite confinement. The study explained the confinement mechanism of the steel tube and the FRP wrap in confined plain or reinforced concrete columns, and the role of steel tube and CFRP wrap in each load stage, which provides a basis for the establishment of a calculation model of the bearing capacity for the columns. The three stages of the confinement mechanism include a steel tube confinement stage which is similar to steel tube confined concrete, and a CFRP-steel tube co-confinement stage in which the total confinement pressure increases rapidly due to the effective co-confinement from steel tube and CFRP wrap, and a FRP-dominated confinement increasing stage when FRP wrap keeps an effective confinement to steel tube and concrete core to resist axial compressive load.

4. Based on previous studies and discussion on the strength models for confined concrete, through a superposition principle considering the confinement of steel tube and CFRP wrap, this paper proposed a simplified calculation model to predict the axial bearing capacity of CFRP-steel tube confined plain concrete and reinforced concrete stub columns. Comparing with test results, the accuracy and

reliability of proposed model was confirmed.

Compared with CFRP, GFRP wrap may be more suitable to work together with the steel tube than CFRP in FRP-STCC elements, because of GFRP materials' low cost, greater fracture strain. The potential galvanic corrosion issues also will be eliminated. In the future, the axial compressive behaviour of GFRP-STCC elements will be investigated.

Acknowledgements

The authors of the paper appreciate the support from the National Key R&D Program of China (No. 2017YFC0703000), the National Natural Science Foundation of China (Nos. 51778102 and 51978126), the Fundamental Research Funds for the Central Universities (No. DUT18LK35), and the Natural Science Foundation of Liaoning Province of China (No. 20180550763).

Notation

A_a cross-sectional area of longitudinal reinforcement
A_c cross-sectional area of concrete core
A_s cross-sectional areas of steel tube
B width of steel tube
B_0 width of concrete core
D equivalent diameter
E_{frp} elastic modulus of FRP
E_s elastic modulus of steel
E_s^t tangent modulus steel in the elastoplastic stage
H height of the specimen
f_a yield strength of longitudinal reinforcement
f_y yield strength of steel tube
f_p proportional limit of steel tube
f_{co} compressive strength of unconfined concrete
f_r confining pressure
$f_{r,s}$ confining pressure provided by steel tube
$f_{r,FRP}$ confining pressure provided by FRP wrap
f_{CF} compressive strength of FRP-confined concrete
f_{CS} compressive strength of steel tube confined concrete
f_{CFS} compressive strength of FRP-steel tube confined concrete
f_{cc1} first peak stress of confined concrete
f_{cc2} ultimate stress of confined concrete corresponding to the rupture of FRP wrap
G shear modulus of the steel
k_1 confinement effectiveness coefficient
k_{s1} shape factor
k_c corner-effect coefficient

k_r reduction factor considering stress concentration at corner
k_ε FRP efficiency factor
n the number of FRP layer
N axial load resisted by the composite column
N_u axial bearing capacity of the composite column
R corner radius
t thickness of steel tube
t_{frp} thickness of FRP wrap
β reduction factor
μ_s Poisson's ratio of steel in the elastic stage
μ_{sp} Poisson's ratio of steel in the elastoplastic stage
σ_h hoop stress of steel tube
σ_v axial stress of steel tube
σ_c axial stress of confined concrete
$\sigma_{h,j}$ hoop stress of a confining jacket
σ_z equivalent stress of steel tube
ε_p equivalent strain of steel tube corresponding to f_p
ε_y equivalent strain of steel tube corresponding to f_y
ε_h hoop strain of steel tube
ε_v axial strain of steel tube
ε_{frp} ultimate tensile strain of FRP coupon
$\varepsilon_{h,rup}$ hoop rupture strain of FRP wrap
ε_{cc1} nominal axial strain of confined concrete corresponding to f_{cc1}
ε_{cc2} nominal axial strain of confined concrete corresponding to f_{cc2}

References

[1] Hu YM, Yu T, Teng JG. FRP-confined circular concrete-filled thin steel tubes under axial compression. J Compos Constr 2011;15(5):850–60.
[2] Xu TX, Liu JP, Wang XD, Guo Y, Chen YF. Behaviour of short CFRP-steel composite tubed reinforced normal and high strength concrete columns under eccentric compression. Eng Struct 2020;205:110096.
[3] Sakaino K, Ishibashi H. Experimental studies on concrete filled square steel tubular short columns subjected to cyclic shearing force and constant axial force. J Struct Constr Eng 1985;353: 81–91.
[4] Xiao Y, Tomii M, Sakino K. Experimental study on design method to prevent shear failure of reinforced concrete short circular columns by confining in steel tube. Trans Japan Concr Inst 1986;8:535–42.
[5] Yan B, Liu J, Zhou X. Axial load behavior and stability strength of circular tubed steel reinforced concrete (SRC) columns. Steel Compos Struct 2017;25(5):545–56.
[6] Aboutaha RS, Machado RI. Seismic resistance of steel-tubed high-strength reinforced-concrete columns. J Struct Eng 1999;125(5):485–94.
[7] Zhou XH, Liu JP, Wang XD, Chen YF. Behavior and design of slender circular tubed-reinforced-concrete columns subjected to eccentric compression. Eng Struct 2016;124:17–28.
[8] Mei H, Kiousis PD, Ehsani MR, Saadatmanesh H. Confinement effects on high-strength concrete. Struct J 2001;98(4):548–53.
[9] Zhou XH, Liu JP. Seismic behavior and shear strength of tubed RC short columns. J Constr Steel Res 2010;66:385–97.
[10] Einde L V D, Zhao L, Seible F. Use of FRP composites in civil structural applications. Constr Build Mater 2003;17(6-7):389–403.

[11] Bai YL, Dai JG, Mohammadi M, Lin G, Mei SJ. Stiffness-based design-oriented compressive stress-strain model for large-rupture-strain (LRS) FRP-confined concrete. Compos Struct 2019;223(2019):110953.
[12] Wang YL, Cai GC, Li YY, Waldmann D, Si Larbi A, Tsavdaridis KD. Behavior of circular fiber-reinforced polymer-steel-confined concrete columns subjected to reversed cyclic loads: experimental studies and finite-element analysis. J Struct Eng 2019;145(9):04019085.
[13] Cao Q, Tao J, Wu Z, Ma ZJ. Behavior of FRP-steel confined concrete tubular columns made of expansive self-consolidating concrete under axial compression. J Compos Constr 2017;21(5):04017037.
[14] Bai YL, Yan ZW, Ozbakkaloglu T, Han Q, Dai JG, Zhu DJ. Quasi-static and dynamic tensile properties of large-rupture-strain (LRS) polyethylene terephthalate fiber bundle. Constr Build Mater 2020;232(2020):117241.
[15] Wang YL, Chen GP, Wan BL, Cai GC, Zhang YW. Behavior of circular ice-filled self-luminous FRP tubular stub columns under axial compression. Constr Build Mater 2020;232(2020):117287.
[16] Wang YL, Wang YS, Wan BL, Han BG, Cai GC, Li ZZ. Properties and mechanisms of self-sensing carbon nanofibers/epoxy composites for structural health monitoring. Compos Struct 2018;200(2018):669–78.
[17] Wang YL, Wang YS, Wan BL, Han BG, Cai GC, Chang RJ. Strain and damage self-sensing of basalt fiber reinforced polymer laminates fabricated with carbon nanofibers/epoxy composites under tension. Compos Part A Appl Sci Manuf 2018;113(2018):40–52.
[18] Zeng JJ, Gao WY, Duan ZJ, Bai YL, Guo YC, Ouyang LJ. Axial compressive behavior of polyethylene terephthalate/carbon FRP-confined seawater sea-sand concrete in circular columns. Constr Build Mater 2020;234(2020):117383.
[19] Cao Q, Tao J, Ma ZJ, Wu Z. Axial Compressive Behavior of CFRP-Confined Expansive Concrete Columns. ACI Struct J 2017;114(2):475–85.
[20] Park JW, Choi SM. Structural behavior of CFRP strengthened concrete-filled steel tubes columns under axial compression loads. Steel Compos Struct 2013;14(5):453–72.
[21] Xiao Y, He W, Choi KK. Confined concrete-filled tubular columns. J Struct Eng 2005;131(3):488–97.
[22] Tao Z, Wang Z, Han L, Uy B. Fire performance of concrete-filled steel tubular columns strengthened by CFRP. Steel Compos Struct 2011;11(4):307–24.
[23] Wang Z, Yu Q, Tao Z. Behaviour of CFRP externally-reinforced circular CFST members under combined tension and bending. J Constr Steel Res 2015;106:122–37.
[24] Yu T, Hu YM, Teng JG. Cyclic lateral response of FRP-confined circular concrete-filled steel tubular columns. J Constr Steel Res 2016;124:12–22.
[25] Park JW, Hong YK, Choi SM. Behaviors of concrete filled square steel tubes confined by carbon fiber sheets (CFS) under compression and cyclic loads. Steel Compos Struct 2010;10(2):187–205.
[26] Liu L, Lu Y. Axial bearing capacity of short FRP confined concrete-filled steel tubular columns. J Wuhan Univ Technol 2010;25(3):454–8.
[27] Teng JG, Hu YM, Yu T. Stress-strain model for concrete in FRP-confined steel tubular columns. Eng Struct 2013;49(2):156–67.
[28] Wang QL, Zhao Z, Shao YB, Li QL. Static behavior of axially compressed square concrete filled CFRP-steel tubular (S-CF-CFRP-ST) columns with moderate slenderness. Thin Wall Struct 2017;110:106–22.
[29] Lin SY. Seismic performance of FRP-steel composite tube confined RC columns. MS Thesis of Harbin Institute of Technology, Harbin, China, 2003. (In Chinese)
[30] Zhao J, Cai GC, Cui L, Si Larbi A, Tsavdaridis DK. Deterioration of basic properties of the materials in FRP-strengthening RC structures under ultraviolet exposure. Polymers 2017; 9(9), 402.
[31] Huang PD. Cyclic axial compression mechanical behavior study of GFRP-steel composite tube confined RC stub columns. MS Thesis of Dalian University of Technology, Dalian, China, 2006. (In Chinese)
[32] GB 50608-2010. Technical code for infrastructure application of FRP composites. Ministry of housing and urban-rural development of the People's Republic of China, 2010. (In Chinese).
[33] GB/T 228-2002. Metallic materials-tensile testing at ambient temperature. General Administration of Quality Supervision, Inspection and Quarantine of the People’s Republic of China, 2002. (In Chinese)

[34] Zhang S, Guo L, Ye Z, Wang Y. Behavior of steel tube and confined high strength concrete for concrete-filled RHS tubes. Adv Struct Eng 2005;8(2):101–16.
[35] Zhang S, Guo L, Tian H. Eccentrically loaded high strength concrete-filled square steel tubes. In: Proceedings of the international conference on advances in structures. Sydney, Australia, 2003.
[36] Chen WF, Saleeb AF. Constitutive equations for engineering materials: Vol.1—Elasticity and modeling. UK: John Wiley & Sons, Inc., 1982.
[37] Wang Z, Wang D, Smith ST, Lu D. CFRP-confined square RC columns. I: Experimental investigation. J Compos Constr 2012;16:150–60.
[38] Pham TM, Hadi MN. Stress prediction model for FRP confined rectangular concrete columns with rounded corners. J Compos Constr 2013;18(1):04013019.
[39] Qi H, Guo L, Liu J, Gan D, Zhang S. Axial load behavior and strength of tubed steel reinforced-concrete (SRC) stub columns. Thin Wall Struct 2011;49(9):1141–50.
[40] Liu J, Zhou X. Behavior and strength of tubed RC stub columns under axial compression. J Constr Steel Res 2010;66(1):28–36.
[41] Mander JB, Priestley MJ, Park R. Theoretical stress-strain model for confined concrete. J Struct Eng 1988;114(8):1804–26.
[42] Lam L, Teng JG. Design-oriented stress-strain model for FRP-confined concrete in rectangular columns. J Reinf Plast Comp 2003;22(13):1149–86.
[43] Lam L, Teng JG. Design-oriented stress-strain model for FRP-confined concrete. Constr Build Mater 2003;17(6-7):471–89.
[44] Hadi MN, Pham TM, Lei X. New method of strengthening reinforced concrete square columns by circularizing and wrapping with fiber-reinforced polymer or steel straps. J Compos Constr 2012;17(2):229–38.
[45] Campione G, Miraglia N. Strength and strain capacities of concrete compression members reinforced with FRP. Cement Concrete Comp 2003;25(1):31–41.

Declaration of Competing Interest

We declare that we do not have any commercial or associative interest that represents a conflict of interest in connection with the work submitted.

CRediT authorship contribution statement

Yanlei Wang: Conceptualization, Funding acquisition, Supervision, Writing - original draft, Writing - review & editing. **Gaochuang Cai**: Conceptualization, Supervision, Writing - original draft, Writing - review & editing. **Amir Si Larbi**: Methodology, Writing - review & editing. **Danièle Waldmann**: Methodology, Validation, Writing - review & editing. **Konstantinos Daniel Tsavdaridis**: Methodology, Validation, Writing - review & editing. **Jianghua Ran**: Data curation, Investigation, Methodology, Validation.